ECS Journal of Solid State
Science and Technology

Perspective—Emergent Phases in Rare Earth Nickelate Heterostructure

ECS Journal of Solid State Science and Technology, 2022 **11** 053004
2162-8777/2022/11(5)/053004/6/$40.00 © 2022 The Electrochemical Society ("ECS"). Published on behalf of ECS by IOP Publishing Limited

Perspective—Emergent Phases in Rare Earth Nickelate Heterostructure

J. Chakhalian[1,z] **and S. Middey**[2,z]

[1]*Department of Physics and Astronomy, Rutgers University, Piscataway, New Jersey 08854, United States of America*
[2]*Department of Physics, Indian Institute of Science, Bengaluru 560012, India*

The prediction of high T_c superconductivity in layers of $LaNiO_3$ through orbital engineering has led to extensive research efforts over the last fifteen years. During this period, a plethora of thin films and heterostructures based rare-earth nickelate family with perovskite structure has been synthesized and explored. In this short perspective, we briefly review the complexity of bulk $RENiO_3$, spotlighting several recent findings of emergent phenomena in heterostructures containing the interface between $RENiO_3$ and another transition metal oxide. Finally, we outline potentially interesting future directions linked to time-domain dynamics to harness new Mott and topological phases in artificial structures of $RENiO_3$.
 [DOI: 10.1149/2162-8777/ac64c3]

Manuscript submitted February 5, 2022; revised manuscript received April 5, 2022. Published May 9, 2022. *This paper is part of the JSS Focus Issue on Focus Issue In Honor of John Goodenough: A Centenarian Milestone.*

The famous volume titled "Magnetism and the Chemical bond" by John B. Goodenough was released in December1964[1] and rapidly earned a reputation of "Atlas Maior" of quantum materials with correlated electrons. Somewhat surprisingly, this encyclopedic compendium contains no mention of rare-earth nickelates despite an early report on the synthesis.[2] However, two years later, in a series of insightful articles on complex oxides with perovskite structure, Goodenough et al., described the majority of structural, electronic, and magnetic properties of these compounds.[3,4] During the 1970s and 80 s, the investigation of rare-earth nickelates based on the chemical formula $RENiO_3$, where *RE* is a rare-earth ion, remained rather dormant until after the discovery of high T_c superconductivity in cuprate oxides with partial perovskite crystal structure.[5] Moreover, since in the periodic table Ni is located next to Cu, there was an active research for the nickel-based high T_c superconducting oxides,[6] which is still ongoing.[7,8] With the renewed interest in nickelates, a massive high-pressure synthesis effort was put forward, finally yielding the complete $RENiO_3$ family that spans from:

La to Lu (see Fig. 1a), thus making the whole family available for the systematic exploration.[9,10]

We begin this perspective article with a brief introduction about the bulk $RENiO_3$ highlighting the complexity of their electronic and magnetic behavior. As shown in the phase diagram of bulk $RENiO_3$ (Fig. 1a), the first member of the nickelate series, $LaNiO_3$ with rhombohedral $R\,\bar{3}\,c$ structure remains metallic down to the lowest probed temperature. The intermediate members with *RE* = Pr and Nd undergo a first order metal-to-insulator transition (MIT) from paramagnetic metallic (PMM) state with orthorhombic (*Pbnm*) structure to an antiferromagnetic insulating (AFI) state accompanied with a lowering of the symmetry to monoclinic ($P2_1/n$).[9,10] For even smaller *RE* ions (e.g., Sm…Lu), as the Ni–O–Ni bond angle decreases further away from the maximal value of ∼165° in $LaNiO_3$, the MIT temperature (T_{MIT}) and magnetic transition (T_N) separate from each other (see Fig. 1). Within the insulating phase, the entire family has a monoclinic ($P2_1/n$) structure with two nonequivalent Ni sites in the unit cell. As for the spin structure, neutron diffraction measurements found the magnetic wave vector to be $(1/2, 0, 1/2)_{ortho}$ [(1/4, 1/4, 1/4) in pseudo cubic notation].[12] The spin arrangement of this *E*'-type antiferromagnetic (*E*'-AFM) phase can be visualized as a sequence of either ↑↑↓↓ or ↑→↓← pseudo-cubic (1 1 1) planes (Fig. 1b). Resonant X-ray scattering (RXS) experiments on single crystalline thin film samples ruled out any orbital ordering[13,14] even though the Ni^{3+} ($t_{2g}^6\ e_g^1$; $S = 1/2$) is expected to be a Jahn-Teller active in a purely ionic picture. RXS experiments further confirmed the existence of spin noncollinearity within the *E*'-AFM phase.[15]

From the electronic structure viewpoint, rare-earth nickelates are multi-band materials, as revealed by the Hall effect and thermopower measurements.[16,17] Recent angle-resolved photoemission studies have also supported this multi-band character.[18–20] In the metallic phase, nickelates behave as a non-Fermi liquid.[21–23] Tunneling measurement also claimed a pseudogap phase in metallic $LaNiO_3$.[24] However, the simultaneous nature of the electronic and structural transitions still remains puzzling. The observation of a magnetic transition for $NdNiO_3$ and $PrNiO_3$ adds further complexity in understanding the mechanism of the MIT. For example, optical conductivity measurements find a gradual opening of a bandgap across the transition through the changes in the electrical resistivity. At the same time, lattice constants show a sharp jump in magnitude across the transition.[25] In addition, the optical band gap (∼ 1 eV) seems much larger than the gap, evaluated from electrical transport data.[26]

Since the insulating phase with monoclinic symmetry consists of two inequivalent Ni, charge disproportionation (CD) [$Ni^{+3} + Ni^{+3} \rightarrow Ni^{+3+\delta} + Ni^{+3-\delta}$] driven insulating phase would have been a natural explanation as the origin of the MIT.[27–30] The observation of two distinct magnetic moments (1.4 μ_B and 0.7 μ_B) in highly distorted $YNiO_3$ supports the CD scenario.[27] However, this conclusion is in contradiction with the magnetic moments of all Ni sites, which are almost identical across the series of $RENiO_3$ with *RE* = Sm, Eu, Pr and Nd.[12,31,32] Complimentarily, the findings of the similar energy dependence of the pseudocubic (1/4 1/4 1/4) magnetic peak across the Ni $L_{3,2}$ edges, observed in RXS experiments across the series with different transition temperatures and structural distortions, is also inconsistent with a conventional CD phase.[33] While a spin density wave (SDW) transition can capture the simultaneous MIT and magnetic transition of $NdNiO_3$ and $PrNiO_3$ and the CD can be a simple consequence of a site-centered SDW transition,[34,35] the appearance of the simultaneous structural transition cannot be accounted for by this mechanism. Though the importance of the electron-electron correlation effect behind the MIT was demonstrated,[36] a pure Mott transition does not require either magnetic or structural transition.

The strong O–Ni covalency and the effective negative charge energy lead to the ground state of Ni ions to be more of $3d^8\underline{L}$ character ($\underline{L}$ denotes a ligand hole antiferromagnetically coupled with the Ni e_g electrons), instead of the ionic $3d^7$ configuration.[37,38] This electronic configuration can easily explain the absence of any orbital ordering with one electron in each e_g state. Considering the dominant contribution of this $3d^8\underline{L}$ configuration, a new CD mechanism has been suggested where the charge redistribution occurs on the oxygen sub-lattice across the MIT.[39] This has been

[z]E-mail: jak.chakhalian@rutgers.edu; smiddey@iisc.ac.in

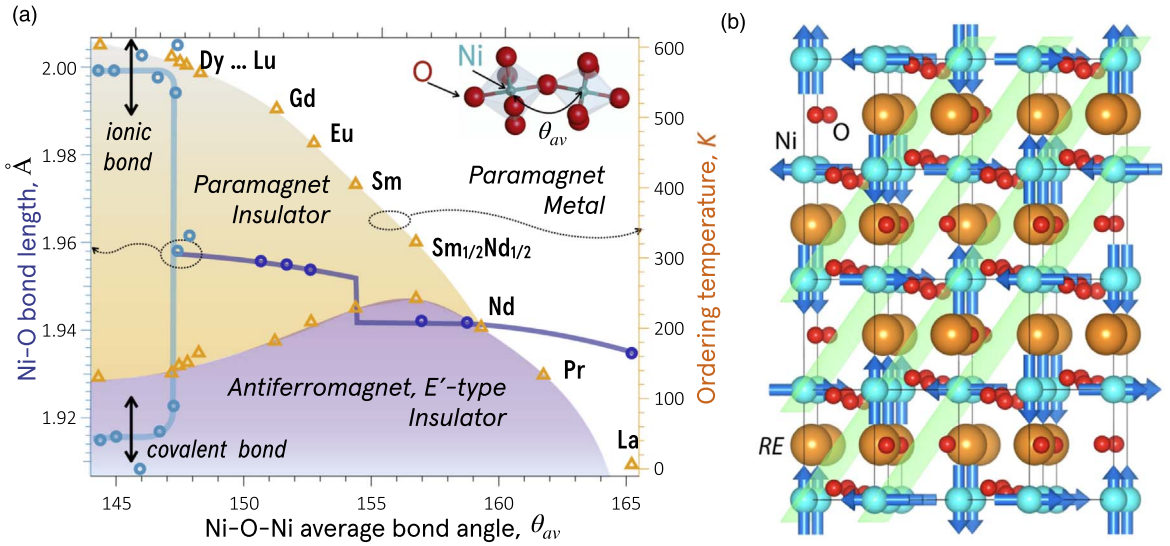

Figure 1. (a) Ni–O bond lengths (left axis) and phase transition temperatures (right axis) have been plotted as a function of Ni–O–Ni bond angle of bulk RENiO$_3$ series. All data have been adapted from Ref. 11 (b) E'-AFM phase with ↑→↓← arrangement of Ni spins. The pseudo-cubic (1 1 1) planes have been shown by green color.

named a bond-disproportionation (BD) transition. Furthermore, this process $3d^8\underline{L} + 3\ d^8\underline{L} \rightarrow 3d^8$ (ionic, $S = 1$) + $3d^8\underline{L}^2$ (covalent, $S = 0$) became known as a site-selective Mott transition.[40–43] Considering the proposed BD scenario, the spin configuration of E'-AFM phase should be thought as a sequence of ↑0 ↓ 0 (1 1 1)$_{pc}$ planes. Remarkably, based on the extensive bond-angle vs. bond-length analysis shown in Fig. 1, Goodenough and collaborators proposed an analogous picture of the bond disproportionation into a periodic pattern of ionic and covalent Ni sites starting around Y–Lu.[11]

Current Status

The continuous advancement in various physical vapor deposition techniques have enabled stabilization of various complex oxides in a single crystalline thin film form with atomic precision.[44–51] This in turn offers a new set of control knobs such as quantum confinement, epitaxial strain, interfacial charge transfer, geometrical lattice engineering etc., to realize a plethora of emergent phenomena.[44–51] The stabilization of single crystalline RENiO$_3$ thin films is highly non-trivial due to the requirement of the +3 high oxidation state of Ni. Moreover, the synthesis of stoichiometric RENiO$_3$ in bulk form requires high oxygen pressure at elevated temperature. As a consequence, only LaNiO$_3$ could be grown as a large single crystal.[27,28,52–54] During the initial synthesis work on nickelate films, it was demonstrated that even though thin films of LaNiO$_3$ can be grown without high oxygen pressure,[55,56] the bulk-like metal-insulator transition could be observed only in NdNiO$_3$ films post annealed under high oxygen pressure.[57] The explanation for the low-pressure film growth was attributed to a coherent film/substrate interface that dramatically lowers the free energy.[58,59] Utilizing this heteroepitaxial stabilization, high-quality single crystalline RENiO$_3$ films with RE = La, Pr, Nd, Sm, Eu on perovskite substrates have been grown under low oxygen partial pressure by pulsed laser deposition,[22,26,60–65] sputtering[66–69] and oxide molecular beam epitaxy.[70–72]

The prediction of potential high T_c superconductivity via orbital engineering[73,74] has resulted in a massive research drive for the growth of various artificial structures (e.g., thin film, heterostructure, superlattice, etc.) of RENiO$_3$, and have been summarized in recent review articles.[75,76] This Perspective article focuses on several recent developments concerning the RENiO$_3$/A_n·B_n··O$_n$··· heterostructure, where A_n·B_n··O$_n$··· represents another transition metal oxide.

***Emergent phases of* RE*NiO$_3$* *through octahedral engineering.*—**When a hetero-interface between two perovskite oxides is formed, there can be a mismatch in lattice constants, octahedral rotational pattern, lattice symmetry, number of electrons on the transition metal site, d orbital configuration, spin ordering pattern, and so on. Collectively, they may lead to novel emergent phenomena. The first group of examples that we describe here, consists of an interface between two members of the RENiO$_3$ series to illustrate how pure structural effects can introduce new phases of matter. From a structural viewpoint, LaNiO$_3$ (LNO) is a special member of the RENiO$_3$ series as it has a different octahedral rotational pattern ($a^-a^-a^-$) compared to the other members ($a^-b^+c^-$).[71,77,78] Since RENiO$_3$ members have a strong tendency to retain their bulk-like symmetry even in thin-film form,[78] a strong structural competition is anticipated at the interface between LNO and other members of RENiO$_3$. This effect has been indeed observed in ultrathin n uc EuNiO$_3$/m uc LaNiO$_3$ [nENO/mLNO] superlattices (here uc is unit cell in pseudocubic notation, n and m = 1, 2).[79–82] The 1ENO/2LNO SL having rhombohedral symmetry remains metallic, whereas the superlattices with $n \geqslant m$ have orthorhombic/monoclinic symmetry and exhibit first-order MIT as a function of temperature. Moreover, resonant scattering experiments have found that the metal phase of 2ENO/1LNO holds monoclinic symmetry.[80] These results demonstrate that the structural symmetry change is not a necessary factor for MIT, thus solving a long-standing puzzle about the origin of MIT. The competition between interfacial unit cell and bulk-like unit cells were further investigated by growing nENO/nLNO SLs (Fig. 2a).[79,83] The SL with n = 8 uc remains metallic, similar to bulk LNO, whereas all short periodic SLs exhibit simultaneous MIT and antiferromagnetic transition (Fig. 2b). Most importantly, thicker bulk-like LaNiO$_3$ layers in these SLs also become antiferromagnetic (Fig. 2c). Moreover, the bond disproportionation (BD) and charge disproportionation (CD) compete with each other within these SLs,[79,83] in contrast to their cooperative nature in bulk RENiO$_3$.[29,84] These emergent behaviors are linked to the fact that LNO layers in short periodic SLs are forced to follow the octahedral tilt pattern of highly distorted ENO layers but have zero or greatly reduced BD (see caption of Figs. 2d–2e for explanation).[83] LNO layers also follow the octahedral rotational pattern of NdNiO$_3$ in NdNiO$_3$/LaNiO$_3$ superlattices.[85] The interfacial length scale is found to be different in the case of NdNiO$_3$/SmNiO$_3$ SLs, signifying the importance of bulk energetics in artificial quantum materials.[86]

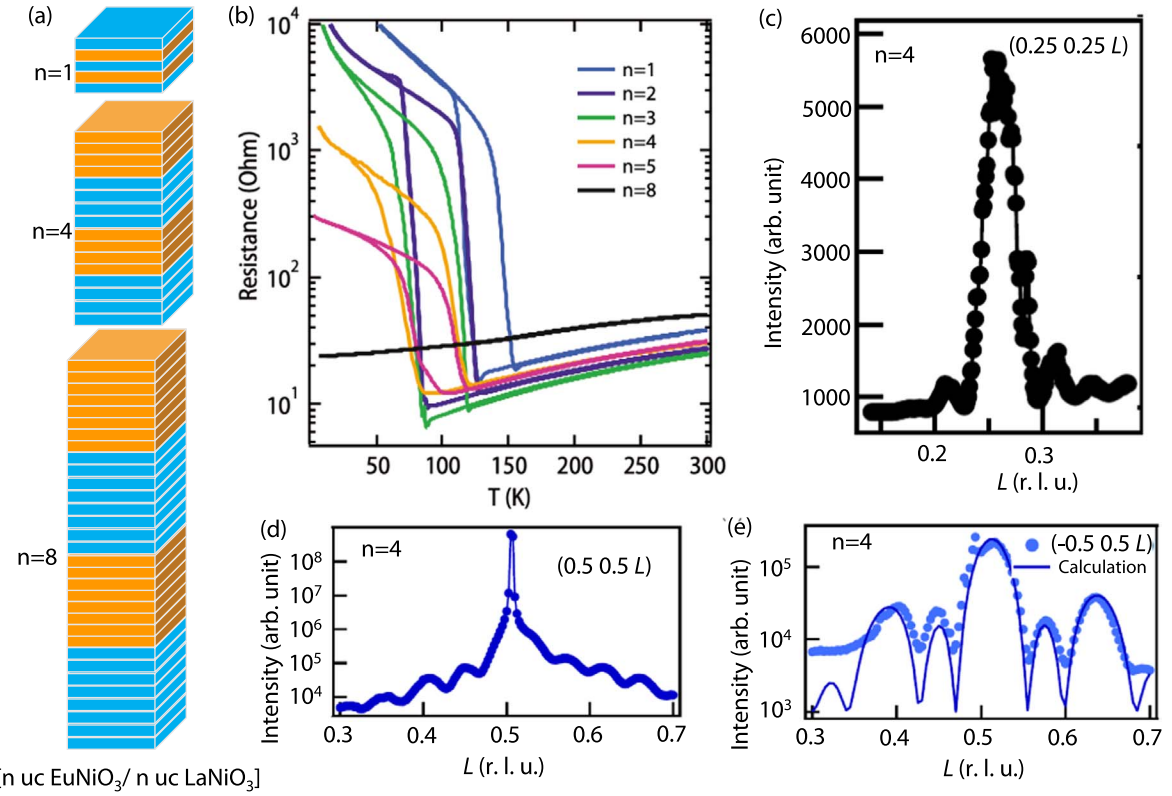

Figure 2. (a) Schematics of deposition sequence for n uc $EuNiO_3$ (ENO)/ n uc $LaNiO_3$ (LNO) superlattice [uc = unit cell in pseudocubic setting]. Cyan and orange color represent ENO and LNO, respectively. (b) Temperature dependent electrical resistivity of n ENO/ n LNO SLs. (c) L scan around (1/4 1/4 1/4) resonant soft X-ray magnetic reflection with the photon energy tuned to the Ni L_3 edge for the $n = 4$ SL. The absence of any satellite along L signifies no magnetic contrast between ENO and LNO layers i.e. the E'-type antiferromagnetic spin arrangement is present throughout the entire film. L scans for the $n = 4$ sample through (d) (1/2 1/2 1/2) and (e) (−1/2 1/2 1/2) reflections. The (1/2 1/2 1/2) peak is allowed for both orthorhombic and monoclinic symmetry but forbidden for rhombohedral symmetry. The absence of any satellite established no significant structural contrast between ENO and LNO. The (−1/2 1/2 1/2) reflection is allowed for monoclinic and forbidden for both orthorhombic & rhombohedral symmetry. The presence of a satellite peak in this case, signifies a contrast in the breathing mode distortion between the ENO and LNO layers. LNO layers have become orthorhombic without (or much suppressed compared to ENO) breathing mode distortion. The data shown in panels (b)–(e) have been adapted from Refs. 79, 83).

***Emergent Phases of* RE*NiO$_3$* *due to interfacial charge transfer.*—**The phenomena due to charge transfer across the interface between two different semiconducting layers remain at the forefront of condensed matter physics. The interesting effects include a p–n junction, two-dimensional electron gas hosting quantum Hall effect, etc. Similar charge transfer physics is being investigated in the case of complex oxide heterostructures. However, the underlying process is more complex due to electron-phonon coupling, strong electron interaction, strong anisotropy of d orbitals, diverse spin orders, etc. Broadly speaking, charge transfer in oxide heterostructures is controlled by two factors: equalization of chemical potential across the interface and the stability of a certain redox pair. For example, in $AB^{+n}O_3/A'B_1{}^{+n_1}O_3$ heterostructures, an electron transfer from ABO_3 to $A'B_1O_3$ can be expected if the pair $B^{+(n+1)}/B_1{}^{+(n_1-1)}$ is more stable than the $B^{+n}/B_1{}^{+n_1}$. Such redox pair-driven charge transfer is short-range and typically limited within the interface's first one/two unit cells.

Since the most stable oxidation state of Ni is +2 and Ni^{4+} is extremely rare, electron doping into the *RE*NiO_3 layers is possible through a sharp interface with other purposely selected perovskites. As a result, such electron transfer can alter orbital and spin configurations, and structural parameters (Ni–O bond lengths and Ni–O–Ni bond angles), resulting in new electronic and magnetic states. Considering the interface between $LaNiO_3$ and Mott insulating $LaTiO_3$ (LTO), Chen et al.[87] predicted electron transfer into $LaNiO_3$ would strongly enhance correlation effects on Ni sites. The follow up experimental work on 2LTO/2LNO superlattice confirmed the interfacial electron transfer ($Ni^{+3} + Ti^{+3} \rightarrow Ni^{+2} + Ti^{+4}$, see Fig. 3) with overall insulating ground state.[88] The charge excitation gap (E_{g1} in Fig. 3) was found to be around 0.2 eV. X-ray absorption spectroscopy measurement determined a charge gap of 1.3 eV between Ti 3d and Ni upper Hubbard band (UHB) state.[88] From these, the correlated gap between UHBs and LHBs (lower Hubbard band) for Ni was deduced to be 1.5 eV. Detailed experimental work on a series of *RE*NiO_3/$GdTiO_3$ heterostructures (*RE* = La, Nd, Sm) further revealed that the hybridization effect of *RE*NiO_3 has a major impact on the electron transfer process.[89] Incorporating polar electric fields along with the charge transfer, a large orbital polarization of Ni was reported using $LaTiO_3/LaNiO_3/LaAlO_3$ heterostructures.[90,91] Since Ti^{+4} with an empty $3d^0$ shell can not donate any electron, no charge transfer has been found in $SrTiO_3$/*RE*NiO_3 heterostructures.[92,93] Similarly, no charge transfer has been seen in $LaFeO_3/SmNiO_3$ heterostructures.[94] This can be readily understood from the fact that Fe^{+3} ($3d^5$) is in a half-filled state and thus highly stable. In both cases,[93,94] the modulation of T_{MIT} has been linked with the change in the octahedral rotational pattern of NiO_6 octahedra near the interfaces.

Several manganite-nickelate heterostructures have been also extensively investigated. In bulk, $CaMnO_3$ is an insulator and undergoes an antiferromagnetic transition around 125 K.[95] As argued before, an interfacial charge distribution would be very unlikely in $LaNiO_3/CaMnO_3$ heterostructure since in $CaMn^{+4}O_3$, Mn has highly stable half-filled t_{2g} orbitals. This simple consideration is consistent with the experiment.[96] The most surprising observation in n uc $LaNiO_3/m$ uc $CaMnO_3$ is ferromagnetism within the first interfacial unit cell of $CaMnO_3$ when the thickness of LNO layers is thick enough to make it metallic.[96] In the absence of any charge transfer, the origin of the unexpected ferromagnetism was

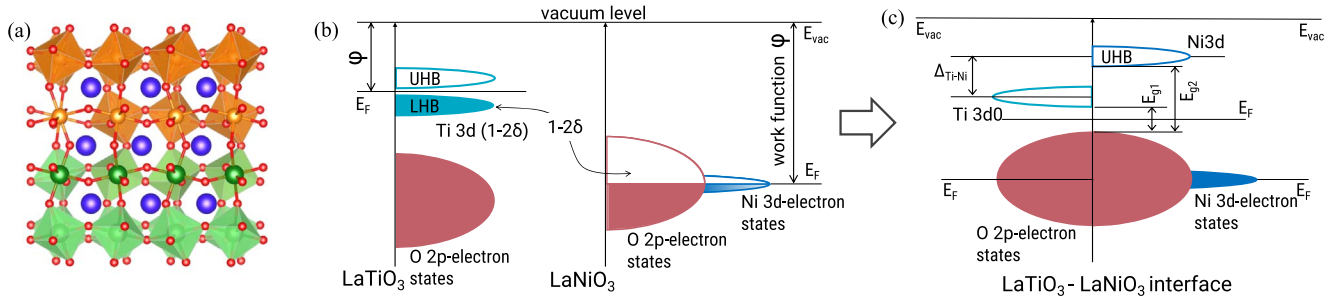

Figure 3. (a) Schematic of 2 uc ABO_3/2 uc $AB'O_3$ superlattice. (b) and (c) Charge transfer between metallic $LaNiO_3$ and insulating $LaTiO_3$ resulting in the formation of a new Mott state at the interface. Adapted from Ref. 88.

explained in terms of double exchange among interfacial Mn ions in the presence of an itinerant electron in the adjacent LNO layers. In contrast, interfacial charge transfer (ICT) is expected in $LaNiO_3/LaMn^{+3}O_3$ (LNO/LMO) interface as the pair Mn^{+4}–Ni^{+2} is more stable than Mn^{+3}–Ni^{+3}. XAS measurements performed on 2 uc LNO/ 2 uc LMO SL indeed found Ni with +2 and Mn with +4 charge states.[97] LNO/LMO SLs grown along[98] direction exhibit exchange bias, which is absent in [001]-oriented SLs.[99] Follow-up XAS measurements revealed that the charge transfer effect is stronger in[98]-[111]-oriented case.[100] Ferromagnetic coupling between Ni and Mn has been confirmed by XMCD (X-ray magnetic circular dichroism) study.[97,100] ICT has been also reported at the interface of nickelates with mixed-valent manganite.[101–104] Among several reports, the most notable observation is the existence of helical spin arrangements within LNO layers, containing atomic-like Ni^{+2} with $3d^8$ electron configuration.[101,102]

Wrobel et al. investigated a series of $La_2CuO_4/LaO/LaNiO_3$ heterostructures to separate the dopant and doped layers from each other.[105] The doped electrons in $LaNiO_3$ result in interfacial charge disproportionation that strongly influences electrical transport behaviors.

All the compounds discussed so far are 3*d* transition metal oxides (TMOs), where the effect of spin–orbit coupling (SOC) is usually disregarded in the determination of the ground state as the crystal field (CF) splitting Δ_{CF} is approximately an order of magnitude larger than the intrinsic SOC λ. However, in 4*d* and 5*d* TMOs, the enhancement of λ makes it comparable to Δ_{CF} As a result of the competing interactions dominated by SOC, several unusual quantum states, including topological insulators, quantum spin liquids, Weyl semimetals, and Kitaev magnets, have been recently predicted.[106] A prototypical example of this class of compounds is the Ruddlesden- Popper (RP) series ($Sr_{n+1}Ir_nO_{3n+1}$, $n = 1; 2; \ldots\infty$) of iridium oxides (Ir^{4+}: $5d^5$). In the layered perovskite Sr_2IrO_4 ($n = 1$), the t_{2g} band is split by the strong SOC leading to the formation of $J_{eff} = 1/2$ and $J_{eff} = 3/2$ subbands. A modest value of the Hubbard *U* further opens a gap and splits the narrow $J_{eff} = 1/2$ band into LHB and UHB, giving rise to a unique spin–orbit entangled Mott-insulating ground state with antiferromagnetic long-range ordering.[107] On the other hand, for the perovskite $SrIrO_3$ ($n = \infty$), the increased Ir 5*d* bandwidth *W*, together with comparable λ and U, eventually prevents a Mott gap opening and results in an intriguing correlated semi-metallic ground state.[108] To validate this idea, Liu et al. investigated $SrIrO_3/LaNiO_3$ superlattices, where a full electron transfer from Ir to Ni was observed, resulting in $S = 1$ spin configurations of interfacial Ni sites.[109] Moreover, the crystal field splitting for the interfacial IrO_6 octahedra was dominant over the SOC, which, together with the Hund's coupling, results in $S = 1$ state of Ir sites. Such suppression of SOC effects through ICT warrants careful checks and reinterpretations of SOC-driven effects in thin films and heterostructures of 5d oxides.

Future Needs and Prospects

Starting with a brief description about bulk *RE*NiO_3 and principle of epitaxial stabilization, we have discussed emergent behaviors of *RE*NiO_3 heterostructures, focusing primarily on octahedral engineering and interfacial charge transfer. In each of these examples, Ni remains in six-fold coordination with oxygen. Interestingly, the local symmetry of Ni can be converted to pyramidal environment through interface engineering and topotactic reduction of *RE*NiO_3-based heterostructure, leading to the observation of large orbital polarization of Ni.[110,111] It would be very interesting to probe electronic and spin reconstruction of such pyramidal NiO_5-units utilizing different members of *RE*NiO_3 series. Apart from interfacial charge doping, additional carriers (either electron or hole) can be introduced in *RE*NiO_3 by chemical substitution[98,112–114] and external electric field.[115–118] While the modulation of MIT of *RE*NiO_3 has been demonstrated using both routes, the underlying mechanism and the effect of carrier doping on BD phase is still missing. Another new direction would be exploring high entropy rare-earth nickelate combining at-least five members of the series in equimolar portion.[65,119]

Due to the presence of simultaneous transitions in *RE*NiO_3, it is highly non-trivial to discern a key order parameter responsible for specific physical properties. This problem has been addressed by the recently developed ultrafast pump-probe technique that explores dynamics of these coupled transitions within a broad time window spanning from femto- to nanoseconds.[120] Taking $NdNiO_3$ as a prototypical system, Stoica et al. optically excited the spin and charge degrees of freedom away from the equilibrium and then used femtosecond soft X-ray pulses to simultaneously probe the recovery dynamics of magnetic and electronic orders including their characteristic timescale (see Fig. 4).[121] In this experiment the authors observed that after the excitation by an optical pump pulse, the magnetism collapses markedly faster than the time scale over which the insulator to metal transition occurs. This observation allowed to exclude magnetism as the prime driver of the MIT. In an another experiment, Abreu et al. investigated the THz conductivity dynamics in $NdNiO_3$ following an optical thermal pump from the insulating ground state into a metastable metallic phase.[122] The application of the THz probe revealed a remarkable contrast between the first (in $NdNiO_3$) and second (in $EuNiO_3$) order dynamics. These early experiments clearly demonstrate the importance of pump-probe experiments to investigate nickelates in the time domain and shed light on controversial or unsolved questions in the equilibrium. Notably, by tracking the characteristic timescales, one can acquire a definitive picture of how charge, magnetic, orbital, and lattice orders emerge and evolve. Moreover, by recording the time evolution of the signals in multiple detection channels, one can figure out the key progenitor for driving the complex transitions. In the future, it would be interesting to examine if dynamic strain engineering can tune the quantum phases. Furthermore, probing and controlling entwined orders can develop into an alternative venue to control these phases with optical stimulation either above or below the band-gap (i.e., electronic vs phonon excitation). For example, it would be intriguing to verify if coherent phonon coupling to spin order during the photo-induced insulator-to-metal transition can substantiate coherence between lattice and magnetic degrees of freedom on picoseconds timescales and at THz speeds.

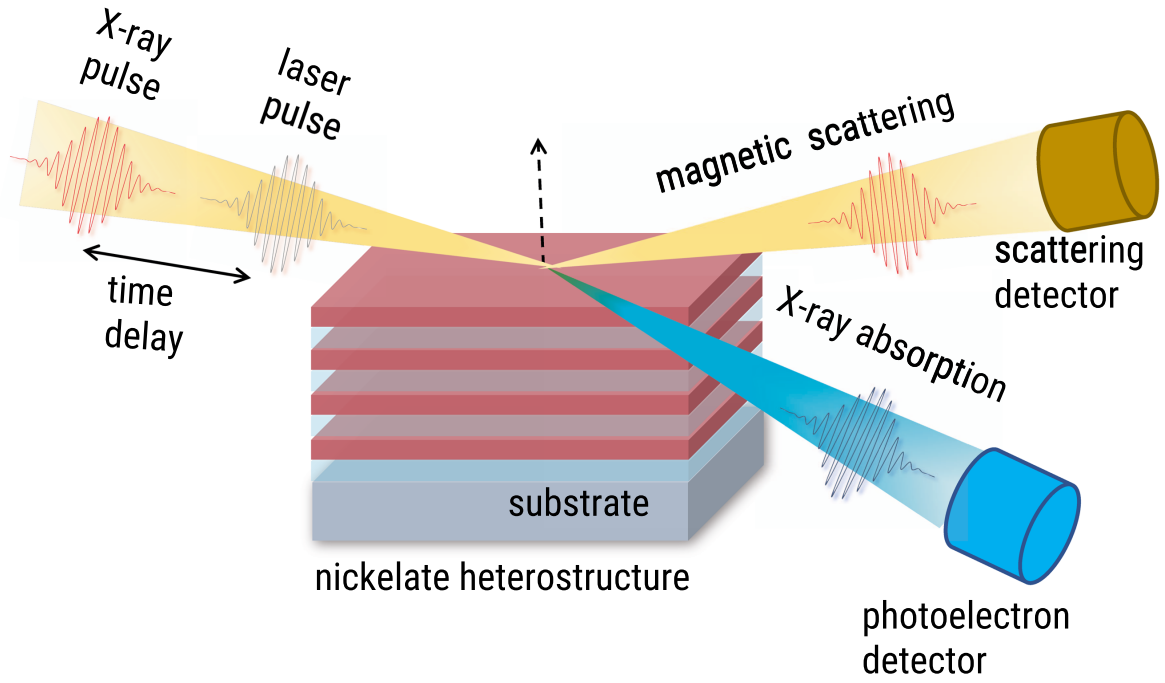

Figure 4. Experimental arrangement of a pump-probe setup, used in Ref. 121.

Conclusions

Overall, it is truly impressive how this particular materials system highlighted by John Goodenough and collaborators almost 60 years ago went through several incarnations only to continue carrying more fascinating stories for future generations of physicists. We believe many more surprises remain hidden in the structures based on rare-earth nickelate, only to be unraveled with the advancement of experimental techniques.

Acknowledgments

This paper is written on the monumental occasion of the centennial birthday of Professor John Goodenough. JC was supported by the U.S. Department of Energy, Office of Science, Office of Basic Energy Sciences under Award Number DE-SC0022160. SM acknowledges financial support of a DST Nanomission grant (Grant No. DST/NM/NS/2018/246) and a SERB Early Career Research Award (Grant No. ECR/2018/001512). JC thanks John W. Freeland (Argonne National Laboratory) and Richard Averitt (University of California, San-Diego) for numerous fruitful discussions on ultra-fast physics of nickelates. We thank Ranjan Kumar Patel and Nandana Bhattacharya for their help during the preparation of the manuscript.

ORCID

S. Middey https://orcid.org/0000-0001-5893-0946

References

1. J. B. Goodenough, *Magnetism and the Chemical Bond* (Interscience publishers) 1 (1963), https://books.google.co.in/books/about/Magnetism_and_the_Chemical_Bond.html?id=ljtRAAAAMAAJ&source=kp_book_description&redir_esc=y.
2. A. Wold, B. Post, and E. Banks, *JACS*, **79**, 4911 (1957).
3. J. Goodenough and P. Raccah, *J. Appl. Phys.*, **36**, 1031 (1965).
4. J. B. Goodenough, *J. Appl. Phys.*, **37**, 1415 (1966).
5. J. B. Torrance, P. Lacorre, A. I. Nazzal, E. J. Ansaldo, and C. Niedermayer, *Phys. Rev. B*, **45**, 8209 (1992).
6. V. I. Anisimov, D. Bukhvalov, and T. M. Rice, *Phys. Rev. B*, **59**, 7901 (1999).
7. D. Li, K. Lee, B. Y. Wang, M. Osada, S. Crossley, H. R. Lee, Y. Cui, Y. Hikita, and H. Y. Hwang, *Nature*, **572**, 624 (2019).
8. W. E. Pickett, *Nature Reviews Physics*, **3**, 7 (2021).
9. M. L. Medarde, *J. Phys. Condens. Matter*, **9**, 1679 (1997).
10. G. Catalan, *Phase Transit.*, **81**, 729 (2008).
11. J.-S. Zhou and J. B. Goodenough, *Phys. Rev. B*, **69**, 153105 (2004).
12. J. L. Garc´ıa-Mu˜noz, J. Rodr´ıguez-Carvajal, and P. Lacorre, *Phys. Rev. B*, **50**, 978 (1994).
13. V. Scagnoli et al., *Phys. Rev. B*, **72**, 155111 (2005).
14. V. Scagnoli, U. Staub, A. M. Mulders, M. Janousch, G. I. Meijer, G. Hammerl, J. M. Tonnerre, and N. Stojic, *Phys. Rev. B*, **73**, 100409 (2006).
15. V. Scagnoli, U. Staub, Y. Bodenthin, M. Garc´ıa-Fern´andez, A. M. Mulders, G. I. Meijer, and G. Hammerl, *Phys. Rev. B*, **77**, 115138 (2008).
16. S. D. Ha, R. Jaramillo, D. M. Silevitch, F. Schoofs, K. Kerman, J. D. Baniecki, and S. Ramanathan, *Phys. Rev. B*, **87**, 125150 (2013).
17. S. K. Ojha et al., *Phys. Rev. B*, **99**, 235153 (2019).
18. R. Eguchi, A. Chainani, M. Taguchi, M. Matsunami, Y. Ishida, K. Horiba, Y. Senba, H. Ohashi, and S. Shin, *Phys. Rev. B*, **79**, 115122 (2009).
19. H. K. Yoo et al., *Sci Rep.*, **5**, 8746 (2015).
20. R. S. Dhaka et al., *Phys. Rev. B*, **92**, 035127 (2015).
21. J.-S. Zhou, J. B. Goodenough, and B. Dabrowski, *Phys. Rev. Lett.*, **94**, 226602 (2005).
22. J. Liu et al., *Nat. Commun.*, **4**, 2714 (2013).
23. C. Liu et al., *Nat. Commun.*, **11**, 1402 (2020).
24. S. J. Allen et al., *APL Mater.*, **3**, 062503 (2015).
25. T. Katsufuji, Y. Okimoto, T. Arima, Y. Tokura, and J. B. Torrance, *Phys. Rev. B*, **51**, 4830 (1995).
26. G. Catalan, R. M. Bowman, and J. M. Gregg, *J. Appl. Phys.*, **87**, 606 (2000).
27. J. A. Alonso, J. L. Garc´ıa-Mu˜noz, M. T. Fern´andez-D´ıaz, M. A. G. Aranda, M. J. Mart´ınez-Lope, and M. T. Casais, *Phys. Rev. Lett.*, **82**, 3871 (1999).
28. J. A. Alonso, M. J. Mart´ınez-Lope, M. T. Casais, M. A. G. Aranda, and M. T. Fern´andez-D´ıaz, *JACS*, **121**, 4754 (1999).
29. U. Staub, G. I. Meijer, F. Fauth, R. Allenspach, J. G. Bednorz, J. Karpinski, S. M. Kazakov, L. Paolasini, and F. d'Acapito, *Phys. Rev. Lett.*, **88**, 126402 (2002).
30. I. I. Mazin, D. I. Khomskii, R. Lengsdorf, J. A. Alonso, W. G. Marshall, R. M. Ibberson, A. Podlesnyak, M. J. Mart´ınez-Lope, and M. M. Abd-Elmeguid, *Phys. Rev. Lett.*, **98**, 176406 (2007).
31. I. Vobornik, L. Perfetti, M. Zacchigna, M. Grioni, G. Margaritondo, J. Mesot, M. Medarde, and P. Lacorre, *Phys. Rev. B*, **60**, R8426 (1999).
32. J. Rodr´ıguez-Carvajal, S. Rosenkranz, M. Medarde, P. Lacorre, M. T. Fernandez-D´ıaz, F. Fauth, and V. Trounov, *Phys. Rev. B*, **57**, 456 (1998).
33. Y. Bodenthin, U. Staub, C. Piamonteze, M. Garcia-Fernndez, M. J. Martnez-Lope, and J. A. Alonso, *J. Phys. Condens. Matter*, **23**, 036002 (2011).
34. S. Lee, R. Chen, and L. Balents, *Phys. Rev. B*, **84**, 165119 (2011).
35. S. Lee, R. Chen, and L. Balents, *Phys. Rev. Lett.*, **106**, 016405 (2011).
36. M. K. Stewart, J. Liu, M. Kareev, J. Chakhalian, and D. N. Basov, *Phys. Rev. Lett.*, **107**, 176401 (2011).
37. S. R. Barman, A. Chainani, and D. D. Sarma, *Phys. Rev. B*, **49**, 8475 (1994).
38. V. Bisogni et al., *Nat. Commun.*, **7**, 13017 (2016).
39. T. Mizokawa, D. I. Khomskii, and G. A. Sawatzky, *Phys. Rev. B*, **61**, 11263 (2000).
40. H. Park, A. J. Millis, and C. A. Marianetti, *Phys. Rev. Lett.*, **109**, 156402 (2012).
41. S. Johnston, A. Mukherjee, I. Elfimov, M. Berciu, and G. A. Sawatzky, *Phys. Rev. Lett.*, **112**, 106404 (2014).
42. A. Subedi, O. E. Peil, and A. Georges, *Phys. Rev. B*, **91**, 075128 (2015).
43. K. Haule and G. L. Pascut, *Sci. Rep.*, **7**, 2045 (2017).

44. D. G. Schlom, L.-Q. Chen, X. Pan, A. Schmehl, and M. A. Zurbuchen, *J. Am. Ceram. Soc.*, **91**, 2429 (2008).
45. L. Martin, Y.-H. Chu, and R. Ramesh, *Materials Science and Engineering: R: Reports*, **68**, 89 (2010).
46. P. Zubko, S. Gariglio, M. Gabay, P. Ghosez, and J.-M. Triscone, *Annu. Rev. Condens. Matter Phys.*, **2**, 141 (2011).
47. H. Y. Hwang, Y. Iwasa, M. Kawasaki, B. Keimer, N. Nagaosa, and Y. Tokura, *Nature Mater.*, **11**, 103 (2012).
48. J. Chakhalian, J. W. Freeland, A. J. Millis, C. Panagopoulos, and J. M. Rondinelli, *Rev. Mod. Phys.*, **86**, 1189 (2014).
49. A. Bhattacharya and S. J. May, *Annu. Rev. Mater. Res.*, **44**, 65 (2014).
50. X. Liu, S. Middey, Y. Cao, M. Kareev, and J. Chakhalian, *MRS Commun.*, **6**, 133 (2016).
51. R. Ramesh and D. G. Schlom, *Nature Reviews Materials*, **4**, 257 (2019).
52. J. Zhang, H. Zheng, Y. Ren, and J. Mitchell, *Crystal Growth & Design*, **17**, 2730 (2017).
53. H. Guo et al., *Nat. Commun.*, **9**, 43 (2018).
54. Y. M. Klein, M. Kozłowski, A. Linden, P. Lacorre, M. Medarde, and D. J. Gawryluk, *Crystal Growth & Design*, **21**, 4230 (2021).
55. K. V. R. Prasad, K. B. R. Varma, A. R. Raju, K. M. Satyalakshmi, R. M. Mallya, and M. S. Hegde, *Appl. Phys. Lett.*, **63**, 1898 (1993).
56. C. Yang, M. Chen, T. Hong, C Wu, J Wu, and T Wu, *Appl. Phys. Lett.*, **66**, 2643 (1995).
57. J. F. DeNatale and P. H. Kobrin, *J. Mater. Res.*, **12**, 2992 (1996).
58. A. R. Kaul, O. Y. Gorbenko, and A. A. Kamenev, *Russ. Chem. Rev.*, **73**, 861 (2004).
59. O. Y. Gorbenko, S. Samoilenkov, I. Graboy, and A. Kaul, *Chem. Mater.*, **14**, 4026 (2002).
60. A. V. Boris et al., *Science*, **332**, 937 (2011).
61. J. Chakhalian et al., *Phys. Rev. Lett.*, **107**, 116805 (2011).
62. D. Meyers, S. Middey, M. Kareev, M. van Veenendaal, E. J. moon, B. A. Gray, J. Liu, J. W. Freeland, and J. Chakhalian, *Phys. Rev. B*, **88**, 075116 (2013).
63. F. Y. Bruno et al., *Phys. Rev. B*, **88**, 195108 (2013).
64. M. Hepting et al., *Phys. Rev. Lett.*, **113**, 227206 (2014).
65. R. K. Patel, S. K. Ojha, S. Kumar, A. Saha, P. Mandal, J. W. Freeland, and S. Middey, *Appl. Phys. Lett.*, **116**, 071601 (2020).
66. J. Son, P. Moetakef, J. M. LeBeau, D. Ouellette, L. Balents, S. J. Allen, and S. Stemmer, *Appl. Phys. Lett.*, **96**, 062114 (2010).
67. S. D. Ha, M. Otaki, R. Jaramillo, A. Podpirka, and S. Ramanathan, *J. Solid State Chem.*, **190**, 233 (2012).
68. A. J. Hauser, E. Mikheev, N. E. Moreno, J. Hwang, J. Y. Zhang, and S. Stemmer, *Appl. Phys. Lett.*, **106**, 092104 (2015).
69. S. Catalano et al., *APL Mater.*, **2**, 116110 (2014).
70. K. R. Nikolaev, A. Bhattacharya, P. A. Kraus, V. A. Vas'ko, W. K. Cooley, and A. M. Goldman, *Appl. Phys. Lett.*, **75**, 118 (1999).
71. S. J. May, J.-W. Kim, J. M. Rondinelli, E. Karapetrova, N. A. Spaldin, A. Bhattacharya, and P. J. Ryan, *Phys. Rev. B*, **82**, 014110 (2010).
72. L. Feigl, B. Schultz, S. Ohya, D. Ouellette, A. Kozhanov, and C. Palmstram, *J. Cryst. Growth*, **366**, 51 (2013).
73. J. c. v. Chaloupka and G. Khaliullin, *Phys. Rev. Lett.*, **100**, 016404 (2008).
74. P. Hansmann, X. Yang, A. Toschi, G. Khaliullin, O. K. Andersen, and K. Held, *Phys. Rev. Lett.*, **103**, 016401 (2009).
75. S. Middey, J. Chakhalian, P. Mahadevan, J. W. Freeland, A. J. Millis, and D. D. Sarma, *Annu. Rev. Mater. Res.*, **46**, 305 (2016).
76. S. Catalano, M. Gibert, J. Fowlie, J. ´I ¯niguez, J.-M. Triscone, and J. Kreisel, *Rep. Prog. Phys.*, **81**, 046501 (2018).
77. A. M. Glazer, *Acta Crystallographica section B*, **28**, 3384 (1972).
78. I. C. Tung, P. V. Balachandran, J. Liu, B. A. Gray, E. A. Karapetrova, J. H. Lee, J. Chakhalian, M. J. Bedzyk, J. M. Rondinelli, and J. W. Freeland, *Phys. Rev. B*, **88**, 205112 (2013).
79. R. K. Patel, D. Meyers, X. Liu, P. Mandal, M. Kareev, P. Shafer, J.-W. Kim, P. Ryan, S. Middey, and J. Chakhalian, *APL Mater.*, **8**, 041113 (2020).
80. S. Middey, D. Meyers, M. Kareev, Y. Cao, X. Liu, P. Shafer, J. W. Freeland, J.-W. Kim, P. J. Ryan, and J. Chakhalian, *Phys. Rev. Lett.*, **120**, 156801 (2018).
81. S. Middey, D. Meyers, S. K. Ojha, M. Kareev, X. Liu, Y. Cao, J. W. Freeland, and J. Chakhalian, *Phys. Rev. B*, **98**, 045115 (2018).
82. S. Middey, D. Meyers, R. Kumar Patel, X. Liu, M. Kareev, P. Shafer, J.-W. Kim, P. J. Ryan, and J. Chakhalian, *Appl. Phys. Lett.*, **113**, 081602 (2018).
83. J.-W. Kim, Y. Choi, S. Middey, D. Meyers, J. Chakhalian, P. Shafer, H. Park, and P. J. Ryan, *Phys. Rev. Lett.*, **124**, 127601 (2020).
84. R. J. Green, M. W. Haverkort, and G. A. Sawatzky, *Phys. Rev. B*, **94**, 195127 (2016).
85. J. Lee, G.-Y. Kim, S. Jeong, M. Yang, J.-W. Kim, B.-G. Cho, Y. Choi, S. Kim, J. S. Choi, and T. K. Lee et al., *ACS Appl. Mater. Interfaces*, **13**, 54466 (2021).
86. C. Dom´ınguez et al., *Nat. Mater.*, **19**, 1182 (2020).
87. H. Chen, A. J. Millis, and C. A. Marianetti, *Phys. Rev. Lett.*, **111**, 116403 (2013).
88. Y. Cao, X. Liu, M. Kareev, D. Choudhury, S. Middey, D. Meyers, J. Kim, P. Ryan, J. Freeland, and J. Chakhalian, *Nat. Commun.*, **7**, 10418 (2016).
89. M. Grisolia et al., *Nat. Phys.*, **12**, 484 (2016).
90. H. Chen, D. P. Kumah, A. S. Disa, F. J. Walker, C. H. Ahn, and S. Ismail-Beigi, *Phys. Rev. Lett.*, **110**, 186402 (2013).
91. A. S. Disa, D. P. Kumah, A. Malashevich, H. Chen, D. A. Arena, E. D. Specht, S. Ismail-Beigi, F. J. Walker, and C. H. Ahn, *Phys. Rev. Lett.*, **114**, 026801 (2015).
92. A. M. Kaiser et al., *Phys. Rev. Lett.*, **107**, 116402 (2011).
93. B. Chen et al., *Nano Lett.*, **21**, 1295 (2021).
94. Z. Liao et al., *Proc. Natl Acad. Sci.*, **115**, 9515 (2018).
95. Z. Zeng, M. Greenblatt, and M. Croft, *Phys. Rev. B*, **59**, 8784 (1999).
96. A. J. Grutter et al., *Phys. Rev. Lett.*, **111**, 087202 (2013).
97. J. Hoffman, I. C. Tung, B. B. Nelson-Cheeseman, M. Liu, J. W. Freeland, and A. Bhattacharya, *Phys. Rev. B*, **88**, 144411 (2013).
98. S.-W. Cheong, H. Hwang, B. Batlogg, A. Cooper, and P. Canfield, *Physica B*, **194**, 1087 (1994).
99. M. Gibert, P. Zubko, R. Scherwitzl, J. Iniguez, and J.-M. Triscone, *Nat. Mater.*, **11**, 195 (2012).
100. C. Piamonteze, M. Gibert, J. Heidler, J. Dreiser, S. Rusponi, H. Brune, J.-M. Triscone, F. Nolting, and U. Staub, *Phys. Rev. B*, **92**, 014426 (2015).
101. J. D. Hoffman et al., *Phys. Rev. X*, **6**, 041038 (2016).
102. G. Fabbris, N. Jaouen, D. Meyers, J. Feng, J. D. Hoffman, R. Sutarto, S. G. Chiuzb˘aian, A. Bhattacharya, and M. P. M. Dean, *Phys. Rev. B*, **98**, 180401 (2018).
103. Z. Xu, S. Hu, R. Wu, J.-O. Wang, T. Wu, and L. Chen, *ACS Appl. Mater. Interfaces*, **10**, 30803 (2018).
104. K. Chen, C. Luo, B. B. Chen, R. M. Abrudan, G. Koster, S. K. Mishra, and F. Radu, *Phys. Rev. Materials*, **4**, 054408 (2020).
105. F. Wrobel et al., *Phys. Rev. Materials*, **2**, 035001 (2018).
106. W. Witczak-Krempa, G. Chen, Y. B. Kim, and L. Balents, *Annu. Rev. Condens. Matter Phys.*, **5**, 57 (2014).
107. B. J. Kim et al., *Phys. Rev. Lett.*, **101**, 076402 (2008).
108. S. J. moon et al., *Phys. Rev. Lett.*, **101**, 226402 (2008).
109. X. Liu et al., *Proc. Natl Acad. Sci.*, **116**, 19863 (2019).
110. Z. Liao et al., *Nat. Commun.*, **10**, 589 (2019).
111. R. A. Ortiz et al., *Phys. Rev. B*, **104**, 165137 (2021).
112. J. Garc´ıa-Mu˜noz, M. Suaaidi, M. Mart´ınez-Lope, and J. Alonso, *Physical Review B*, **52**, 13563 (1995).
113. P.-H. Xiang, S. Asanuma, H. Yamada, I. Inoue, H. Akoh, and A. Sawa, *Appl. Phys. Lett.*, **97**, 032114 (2010).
114. J. Shi, Y. Zhou, and S. Ramanathan, *Nat. Commun.*, **5**, 1 (2014).
115. S. Asanuma et al., *Appl. Phys. Lett.*, **97**, 142110 (2010).
116. R. Scherwitzl, P. Zubko, I. G. Lezama, S. Ono, A. F. Morpurgo, G. Catalan, and J.-M. Triscone, *Adv. Mater.*, **22**, 5517 (2010).
117. S. Bubel, A. J. Hauser, A. M. Glaudell, T. E. Mates, S. Stemmer, and M. L. Chabinyc, *Appl. Phys. Lett.*, **106**, 122102 (2015).
118. S. D. Ha, U. Vetter, J. Shi, and S. Ramanathan, *Appl. Phys. Lett.*, **102**, 183102 (2013).
119. C. M. Rost, E. Sachet, T. Borman, A. Moballegh, E. C. Dickey, D. Hou, J. L. Jones, S. Curtarolo, and J.-P. Maria, *Nat. Commun.*, **6**, 8485 (2015).
120. M. F¨orst, C. Manzoni, S. Kaiser, Y. Tomioka, Y. Tokura, R. Merlin, and A. Cavalleri, *Nat. Phys.*, **7**, 854 (2011).
121. V. Stoica et al., *arXiv preprint arXiv* (2020).
122. E. Abreu, D. Meyers, V. K. Thorsmølle, J. Zhang, X. Liu, K. Geng, J. Chakhalian, and R. D. Averitt, *Nano Lett.*, **20**, 7422 (2020).